Journal of Achievements in Materials and Manufacturing Engineering
VOLUME 28
ISSUE 2
June
2008

The structure of austenitic steel AISI 316 after ECAP and low-cycle fatigue

M. Greger [a,*], V. Vodárek [a], L.A. Dobrzański [b], L. Kander [c], R. Kocich [a], B. Kuřetová [a]
[a] Faculty of Metallurgy and Materials Engineering, VŠB - Technical University of Ostrava, 17. listopadu 15, 708 33 Ostrava – Poruba, Czech Republic
[b] Division of Materials Processing Technology, Management and Computer Techniques in Materials Science, Institute of Engineering Materials and Biomaterials, Silesian University of Technology, ul. Konarskiego 18a, 44-100 Gliwice, Poland
[c] VÍTKOVICE – Research and Development, Pohraniční 693/31, 706 02 Ostrava – Vítkovice, Czech Republic
* Corresponding author: E-mail address: miroslav.greger@vsb.cz

Received 24.04.2008; published in revised form 01.06.2008

Properties

ABSTRACT

Purpose: The article presents results of investigation of structure and properties of austenitic steel grade AISI 316 after application of Equal Channel Angular Pressing (ECAP) at the temperature of approx. 290ºC.
Design/methodology/approach: The ECAP method led to significant improvement of strength of investigated material. Experiments were planned and realised at the temperature ranging from room temperature up to above mentioned temperature.
Findings: It was established with use of the EBSD technique that after 8 passes through the ECAP die the sub-grains with an angle of disorientation smaller than 10º formed less than 20% of resulting structure. Average size of austenitic grains with high angle boundary after 8 passes was approx. 0.32 µm. It was proven that the ECAP method enables obtaining of ultra fine-grained austenitic structure formed by recrystallised grains with very low density of dislocations.
Practical implications: The Technology ECAP was applied on austenitic steel AISI 316. It was verification of ECAP application possibility on steel AISI 316 importantly for following applying on similar kinds of steel, because ECAP technology influence on fatigue properties was confirmed.
Originality/value: It can be predicted on the basis of obtained results that, contrary to low-cycle fatigue the ultra-fine grained material will manifest at fatigue load in the mode of constant amplitude of stress higher fatigue characteristics, particularly fatigue limit.
Keywords: Structure; Low-cycle fatigue; Steel AISI 316; ECAP

1. Introduction

It is well known a positive influence of ECAP technology on final material properties namely non ferrous metals but steel as well. However not many works is focused on achieved fatigue properties after that treatment. This paper wants to contribute to knowledge distribution about austenitic stainless steel AISI 316 behaviour under ECAP.

2. Experimental

Series of samples made of austenitic stainless steel AISI 316 was processed by the ECAP technology. Basic chemical composition is given in the Table 1 and mechanical properties in the Table 2. The samples were manufactured with the following dimensions: ϕ 12 mm, length 60 mm. They were pushed through the ECAP matrix by 2 to 8 passes [1]. Matrix had channel

Table 1.
Basic chemical composition of steel

C	Mn	Si	P	S	Cu	Ni	Cr	Mo
0.03	1.64	0.18	0.011	0.007	0.06	12.5	17.6	2.4

Table 2.
Mechanical properties of the steel AISI 316 before ECAP (20 °C)

Steel grade	E, GPa	$R_{p0.2}$, MPa	R_m, MPa	A, %	Z, %	KV, J	HB
AISI 316	216	330	625	45	-	90	210

diameter 12 mm and angle 105° (Fig. 1). Pressure in the matrix varied around approx. 740 MPa. Temperature of extrusion varied from room temperature up to 280°C. After extrusion material was taken from the samples for metallographic testing and testing bars were manufactured for testing of mechanical properties.

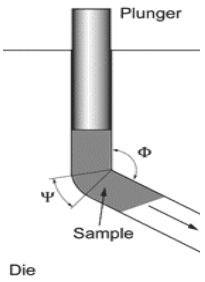

Fig. 1. Scheme of the ECAP process

In order to expand the existing findings the testing bars were exposed to intensive magnetic field and impact of magnetic field on change of mechanical properties was investigated by tensile test. The sample was after eight passes subjected to structural analysis.

Ten samples were determined for investigation of influence of the ECAP technology on fatigue properties. Individual samples were subjected to different number of passes: 3 pieces had 4 passes, 4 pieces had 5 passes and 3 pieces had 6 passes. Test samples for testing of low-cycle fatigue had diameter of the measured part 5 mm and overall length 55 mm, Figure 2.

The amplitude of plastic deformation was the key factor for control of fatigue process. The following Equation was used for the dependence $\varepsilon_{ap} - N_f$ [3, 4]:

$$\varepsilon_{ap} = \varepsilon_f' (2N_f)^c \quad (1)$$

where ε_f' is coefficient of fatigue ductility, c is exponent of the service life curve.

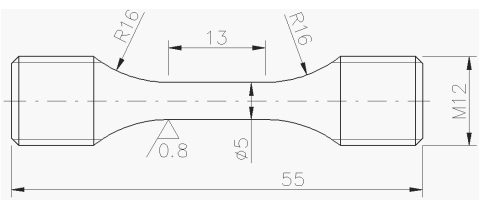

Fig. 2. Testing specimen for test of low-cycle fatigue [2]

3. Results and their analysis

3.1. Structure

Microstructure of steel was formed by equiaxed grains of austenite, which was discontinuously bordered by carbidic particles, shown in the Figure 3. Small formations of decomposed carbidic component were present in very small quantity at the boundaries of austenite grains. Small particles of precipitates were observed also inside austenite grains. Medium size of austenite grains was approx. 35μm.

Structures were analysed from the viewpoint of the course of strengthening and restoring processes. Figure 3 documents deformed sub-structure of the steel AISI 316 after ECAP deformation by 4 to 8. Metallic matrix contained sub-grains of uneven size. Size of sub-grains was in most cases smaller than 0.1 μm, only exceptionally some sub-grains/grains of the size of approx. 0.5 μm were observed. Density of dislocations in metallic matrix was very high, presence of particles of precipitate was not found. In cases when neighbouring grains showed approximately identical diffraction contrast, it can be expected that angle of disorientation is only several degrees, while in case of significant changes of contrast rather high angular disorientation is probable. Figure 3 documents a diffraction pattern, which was obtained from the area with diameter of approx. 1 μm. Occurrence of discontinuous circles and at the same time asimuthal blurring of diffraction traces evidences the fact that big amount of fine sub-grains/grains with more or less different crystallographic orientation was present in the investigated area.

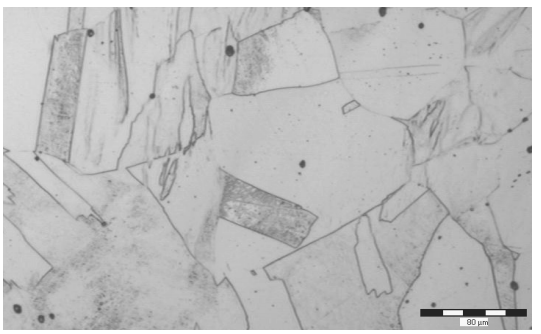

Fig. 3. Original structure of steel AISI 316

Austenitic matrix often contained deformation bands, which were formed during the ECAP deformation, see Figure 4. Deformation bands in austenitic steels can be formed by irregularly overlapping tiered errors, deformation twins or ε-martensite [5-7]. These deformation bands are formed along octahedral planes {111}γ of austenitic matrix. It was proved with use of electron microscopy that in majority of cases these are deformation twins, nevertheless, presence of distinct stretching of reflections intensity („streaking") in directions {111}γ proves frequent occurrence of crystallographic defects in these formations [8-11]. Width of deformation bands was very variable. In some areas intersecting systems of deformation bands occurred, which were formed at several planes of the type {111}, see Figure 4 [12].

Points of intersection of deformation bands generally represent preferential points for formation of particles of α'-

martensite. However, electron diffraction analysis did not confirm occurrence of α'- martensite in these areas [13-17]. Occurrence of α'- martensite in investigated sample was not confirmed even by X-ray diffraction analysis [18-20]. Deflection (deformation) of deformation bands was in many cases quite distinctly visible in pictures in light field [21]. This evidences the fact that deformation bands formed during the ECAP deformation were further deformed during next passes. Sub-grains with high density of dislocations were usually aligned along deformation bands.

Microstructure of steel after 4 ECAP passes was non-homogenous, original austenitic grains were largely deformed. Largely deformed austenitic grains forming directed bands are clearly visible in the Figure 3. Sub-structure was present inside austenitic grains, distribution of carbidic particles remained unchanged. Micro-structure of steel after 6 ECAP passes, see in the Figure 5.

After 6 passes of ECAP went statical recrystalization annealing 800^{o}C/0.5 h. The structure after annealing is shown in Figure 6.

The TEM analysis proved that original equiaxed austenitic grains were replaced by stretched sub-grains/grains of variable size. Sub-grains/grains formed usually directed parallel bands, see the Figure 7. Important local differences of diffraction contrast indicated that disorientation angles between individual sub-grains/grains were highly variable. Density of dislocations inside individual stretched austenitic sub-grains/grains was usually comparatively high, or arrangement of dislocations into dislocation walls was observed. Small grains with well defined boundaries and low density of dislocations were observed locally. It can be therefore assumed that formation of fine-grained structure was influenced not only by mechanisms of fragmentation of deformed grains, but also by re-crystallisation processes.

It was established at the TEM analysis of the sample after 8 ECAP passes, that increase of number of passes resulted in improvement of uniformity and fineness of grains of resulting structure. This is result of synergic effect of the applied temperature of pressing, total true deformation and latent heat generated by the severe plastic deformation. Diffraction contrast of some adjacent sub-grains/grains was very similar, while in other cases it was very different. This indicates that structure is formed by a mixture of sub-grains with very low value of the angle disorientation and also grains separated by high-angle boundaries.

Density of dislocations inside sub-grains/grains was mostly very low, boundaries of sub-grains/grains were well defined (Fig. 8). Majority of sub-grains/grains was equiaxed, however, in some areas significantly stretched sub-grains/grains were observed. Results of the TEM analysis confirm, that recrystallisation processes influenced significantly formation of the ultra fine-grained austenitic structure.

Size of some sub-grains/grains was smaller than 0.1μm, size of other ones was bigger than 0.5μm [22]. Globular particles of carbides were present at boundaries of some austenitic grains. It can be assumed that these carbidic particles have a positive effect on stabilisation of ultra fine-grained austenitic structure against coarsening. Typical examples of sub-structure of the sample after 8 ECAP passes are shown in the Figure 9.

Understanding of mechanism of formation of austenitic grains in deformed samples as well as objective assessment of the size of grains with high-angle boundary requires information about mutual angle disorientation of individual sub-grains/grains. Ideal experimental technique for obtaining these data is at present the FEG SEM in combination with the EBSD [23]. This technique enables determination of crystallographic orientation (Miller index of the line perpendicular to the sample surface) at any place on the sample surface on the basis of the Kikuchi lines, formed by the mechanism of flexible diffusion of originally inflexibly diffused electrons right before the surface of heavily inclined sample [24]. Mapping of crystallographic orientation of the sample surface can be done with a minimum step of 0.1 μm.

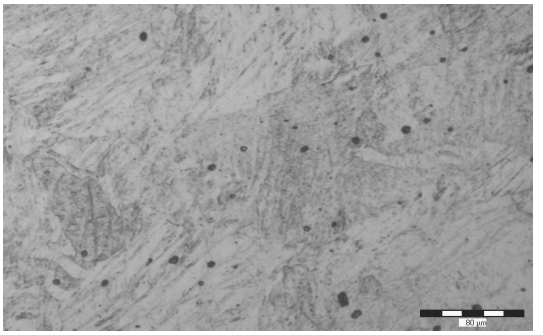

Fig. 4. Microstructure of the sample after 4 ECAP passes

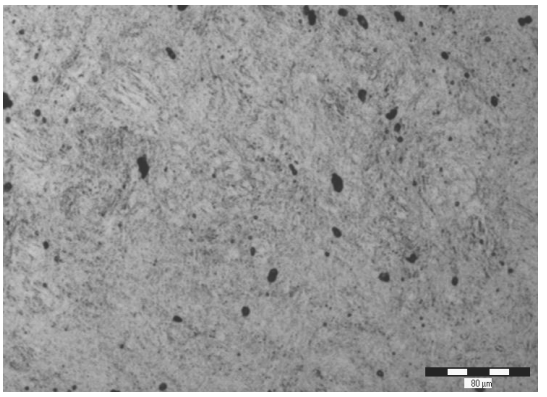

Fig. 5. Microstructure of the sample after 6 ECAP passes

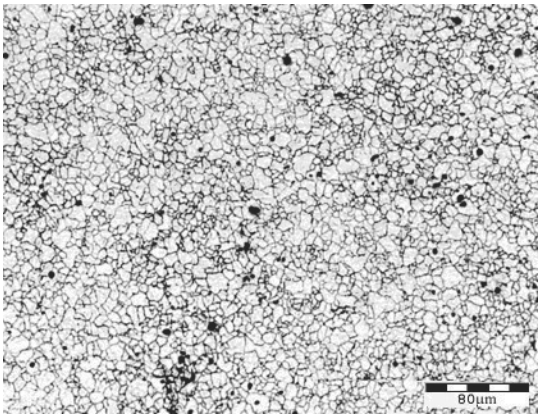

Fig. 6. Microstructure of the sample after 6 ECAP passes and after recrystalization annealling

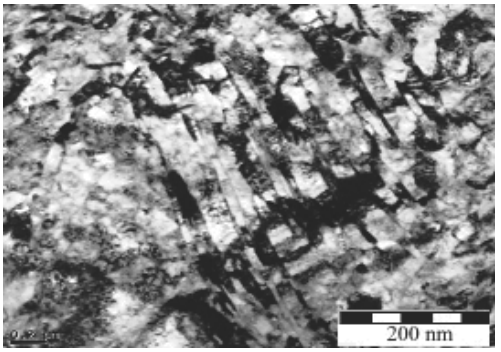

Fig. 7. Substructure of sample after 6 passes

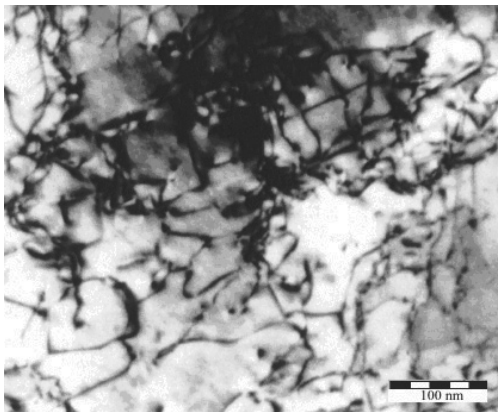

Fig. 8. Dislocation substructure after 6 passes ECAP

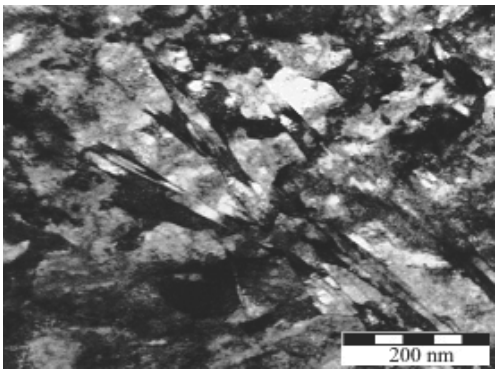

Fig. 9. Substructure of sample after 8 passes

EBSD results obtained on the sample after 8 ECAP passes were processed in the form of crystal orientation maps (COM), where the areas of various orientation on the sample surface are discriminated by different colouring. The obtained results were further processed by computers as follows:

a. in the areas, where the disorientation angle of adjacent pixel was greater than 2°, the boundaries were plotted. In this manner boundaries of sub-grains were visualised, as well as boundaries of grains with high-angle boundary;
b. in order to differentiate between the sub-grains and grains the boundaries of grains were plotted only in the areas, where disorientation of adjacent pixels exceeded 10°;
c. grain boundaries were plotted in the areas, where disorientation of adjacent pixels exceeded 20°.

Map of crystal orientations (COM), shown in the Figure 10, documents large quantity of differently oriented sub-grains/grains in the investigated area.

The Figure 11 shows the boundaries generated in the areas, where the angle disorientation between the adjacent pixels was at least 2°.

If we define sub-grains as areas with the maximum angle disorientation of 10°, it is possible to discern the sub-grains from the grains with high-angle boundaries by comparing the Figures 12 and 13.

It was found that in some cases the angle disorientation of part of perimeter of one grain corresponded to a sub-grain, and the rest of the perimeter was a boundary with high-angle orientation.

The Figure 13 documents a distribution of grains in the investigated area with the angles of disorientation exceeding 20°.

Results of statistic processing of angle disorientation of sub-grains and grains in the sample after 8 ECAP passes are shown in the Figure 14. It is obvious that sub-grains with the angle of disorientation under 10° formed only approx. 15% of all austenitic grains. This confirms the fact that majority of austenitic grains was formed by the mechanism of recrystallisation. No preferential occurrence of special boundaries was observed in the area of high-angle boundaries, such as e.g. twin boundaries.

The biggest share of sub-grains corresponded to the angles of disorientation up to 4°.

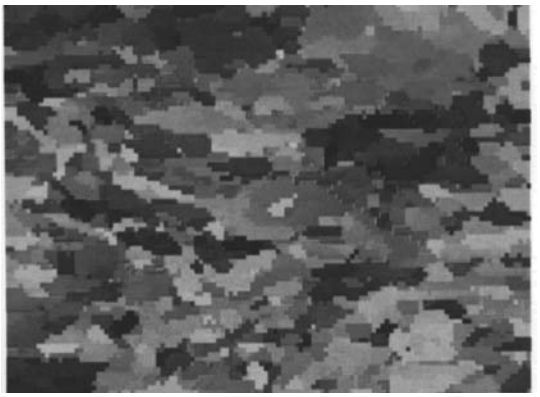

Fig. 10. Crystall oriented map, sample after 8 ECAP passes

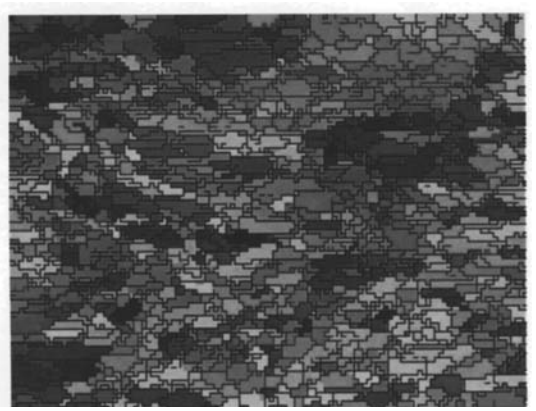

Fig. 11. Grain boundaries with angle dezorientation digger than 2°, sample after 8 ECAP passes

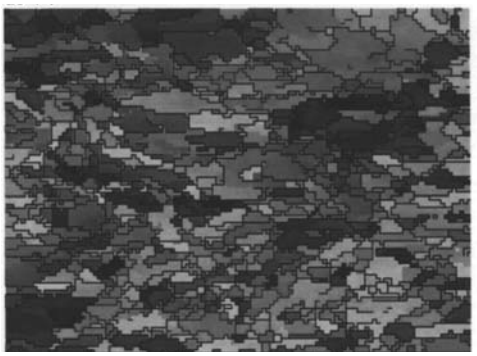

Fig. 12. Grain boundaries with angle dezorientation digger than 10°, sample after 8 ECAP passes

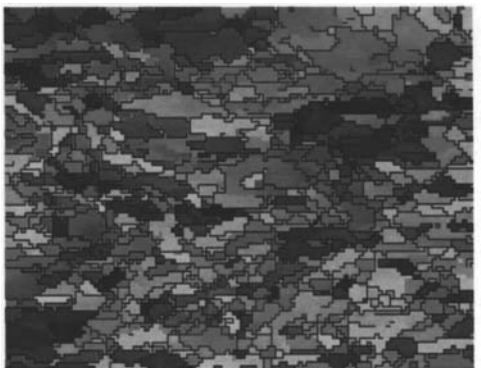

Fig. 13. Sub/Grain boundaries with angle dezorientation digger than 20°, sample after 8 ECAP passes

In conformity with data from literature it can be presumed that influence of sub-grains on the level of mechanical properties of investigated steel is lower than in case of the grains of high-angle boundaries. Important in this connection is the fact that majority of ultra fine-grained austenitic grains in the structure was separated by high-angle boundaries.

Histogram of size distribution (equivalent average) of the grains with high-angle boundaries is shown in the Figure 15.

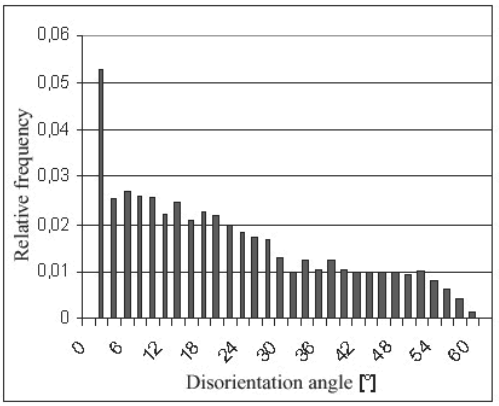

Fig. 14. Angle disorientation of sub-grain and grain boundaries, sample after 8 ECAP passes

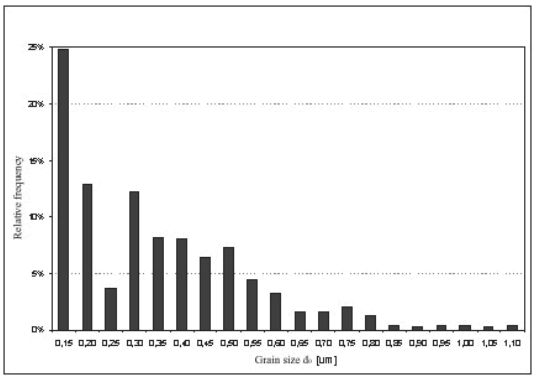

Fig. 15. Size distribution of grains with high-angle boundaries, sample after 8 ECAP passes

After 8 ECAP passes approximately 25% of all grains was in the lowest size class (0.1-0.15 μm). On the other hand size of some austenitic grains was bigger than 1μm. It is obvious from results of the TEM analysis, that many grains were smaller than the smallest usable step at the EBSD analysis (0.1 μm). Medium size of grains with the angle of disorientation greater than 10° was 0.32±0.20 μm. This is only orientational result, since grains with the size smaller than 0.1 μm could not be included into this analysis.

The results obtained at the analysis of influence of severe plastic deformation by the ECAP method on structure of austenitic steel can be summarised as follows:

a. Deformation of investigated steel by the ECAP method at the temperature of approx. 290°C lead to important improvement of strength properties. The biggest increase in strength was found after the first two passes through the ECAP die;
b. Deformation occurred after 8 ECAP passes lead to formation of ultra fine-grained austenitic structure with small share of globular carbidic particles, which were usually present at the boundaries of austenitic grains. Density of dislocations inside austenitic grains was very low. Majority of austenitic grains was formed by the mechanism of re-crystallisation of deformed metallic matrix;
c. Sub-grains with an angle of disorientation under 10° formed after 8 ECAP passes only approximately 15% of all austenitic grains;
d. Medium size of austenitic grains with high-angle boundary after ECAP passes was 0.32±0.20 μm. However, the anis could not include the grains, the size of which was smaller than 0.1 μm. In comparison with the initial structural state the grain size was refined by two orders.

3.2. Mechanical properties

Samples after ECAP with number of passes (4, 6, 8) were used for investigation of influence of the ECAP technology on fatigue properties of the steel AISI 316 with special focus on the area of low-cycle fatigue. Altogether 10 samples were prepared, 3 pieces after 4 passes, 4 pieces after 5 passes and 3 pieces after 6 passes.

Modified testing specimens for testing of low-cycle fatigue, with diameter of the measured part 5 mm and length 55 mm were made from these samples. In order to expand the existing findings the testing bars were exposed to intensive magnetic field and impact of magnetic field on change of mechanical properties was investigated by tensile test Results of tensile testing, which were used for investigation of impact of intensive magnetic field on mechanical properties are given in the Table 3.

Table 3.
Influence of magnetic field on mechanical properties of the steel AISI 316

Designation	E [MPa]	$R_{p0.2}$ [MPa]	R_m [MPa]	Z [%]
1	190837	271.3	586.2	80.6
2	200717	280.6	586.2	80.6
Magnetic field	188276	283.1	588.5	81.5
Magnetic field	201817	278.4	587.6	80.6
Magnetic field	195199	282.1	592.0	80.8

It follows from results of tensile tests that influence of magnetic field on mechanical properties determined by tensile test was not confirmed in investigated material. Minor differences in individual mechanical properties can be attributed to the scatter of mechanical properties within the frame of poly-crystalline materials.

Mechanical properties change in dependence on numbers of passes, strength properties ($R_{p0.2}$ and R_m) distinctly increase, plastic properties described by narrowing almost do not change (Table 4). Intensity of increase in $R_{p0.2}$ and R_m is shown in the Figure 16.

Micro-structural condition for increase of strength properties in investigated steel is fine grain and its stability. Several methods for grain refining and limitation of its growth are known at present – phase transformations, re-crystallisation, big plastic deformations (deformation of alloys with duplex structure, distribution of phases in duplex alloys, dispersion segregated particles), etc. Selection of methods of grain refining and slowing of its growth is in individual cases given by state and properties of structure.

Increasing of strength properties in dependence on grain size is determined by the Hall-Petch relation:

$$\sigma_y = \sigma_0 + k_y d^{-1/2} \quad (2)$$

where: σ_0 = the particle friction stress, and it is the yield stress for the limit $d \to \infty$, k_y = the slope of the line and it is known as the dislocation locking parameter, which represents the relative hardening contribution due to grain boundaries.

For ordinary grade the following values are usually given σ_0=70 – 104 MPa and k_y = 18.1 MPa $mm^{1/2}$.

3.3. Tests of low-cycle fatigue

Testing specimens for determination of the Manson – Coffin curve and curve of deformation strengthening were prepared from extruded samples after 2 to 6 ECAP passes. Apart from extruded samples the initial state was tested as well. The aim was to determine influence of number of ECAP passes on shape and position of the Manson-Coffin curve and curve of deformation strengthening. Altogether 10 samples were processed after application of the ECAP technology (3 samples after 4 passes and 6 samples after and 4 samples after 5 passes) and 12 samples with initial structure.

Test of low-cycle fatigue was performed according to the standard ASTM E 606 at laboratory temperature on servo-hydraulic testing equipment MTS 100 kN by „hard" method of load in alternate traction – pressure. During these tests a constant amplitude of total deformation ε_{ac} was preserved. Tests of low-cycle fatigue were realised at constant rate of total deformation ε_{ac} = 4.10^{-3} s^{-1}. Longitudinal deformation of testing specimens was read by the sensor MTS 632-42C-11 with the basis 12 mm.

Table 4.
Change of mechanical properties of steel AISI 316 after the 2nd to 5th pass

Number of ECAP passes	$R_{p0.2}$ [MPa]	R_m [MPa]	E [MPa]	A [%]	Z [%]
Initial state	330	590	190 000	60	-
2	899	916	179 215	22	68
3	970	998	180 125	15	60
4	1 063	1 099	179 819	15	60
5	1 103	1 140	182 028	15	60

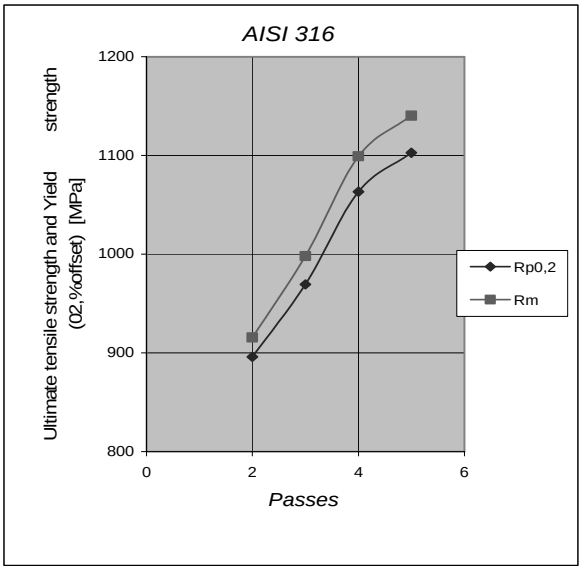

Fig. 16. Influence of number of passes on strength properties of steel AISI 316

During loading of individual testing specimens hysteresis curves were read and recorded (dependence stress – deformation), from which after rupture of individual testing specimens the level of elastic (ε_{ael}) and plastic deformation (ε_{apl}) for $N_f/2$ was evaluated.

After completion of each test the number of cycles till rupture N_f was recorded and from hysteresis curve for approximately N = $N_f/2$ for the chosen amplitude of total deformation ε_{ac} there were deducted amplitude of plastic deformation ε_{apl}, amplitude of elastic deformation ε_{ael} and amplitude of stress σ_a. Curves of service life expressed in the form were plotted from experimental data:

$$\varepsilon_{ac} = \varepsilon_{ael} + \varepsilon_{pl} = \frac{\sigma'_f}{E}(N_f)^b + \varepsilon_f (N_f)^c \quad (3)$$

Cyclic curves stress-deformation were also determined for complex assessment of response of steel after the ECAP to alternating plastic deformation in traction – pressure:

$$\sigma_a = k \cdot \varepsilon_{apl}^n \quad (4)$$

Manson-Coffin curves of service life were plotted from the obtained values, as well cyclic curve of deformation strengthening. These values characterise deformation behaviour of material for

prevailing time of its fatigue service life and they are therefore material characteristics. Results of individual test of low-cycle fatigue were processed in a form of graphic diagrams (Figures 17 to 19). The influence of individual passes to magnitude values in Equations (3) and (4) are pointed out (Table 5).

Table 5.
The magnitude values in Equations (3) and (4)

	As received	4 passes	5 passes	6 passes
σ'_f / E	0.0092	0.0117	0.0255	0.0296
b	-0.01838	-0.1389	-0.2188	-0.2431
ε_f	0.21	0.3327	0.7848	0.328
c	-0.457	-0.7444	-0.8935	-0.8338
k	1729.5	1791.0	2771.3	3620.0
n	0.3026	0.1538	0.186	0.2194

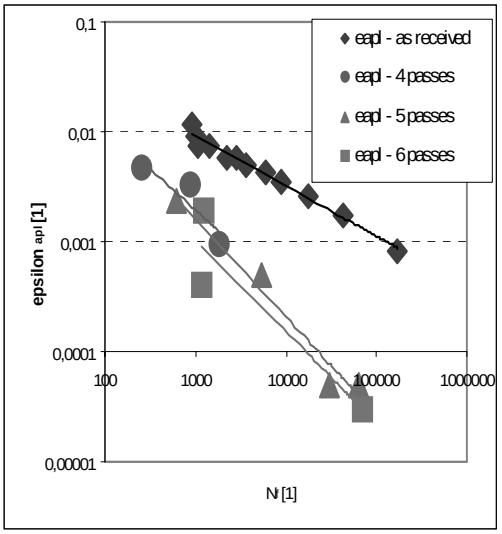

Fig. 17. Curves of low-cycle fatigue $\varepsilon_{apl} - N_f$

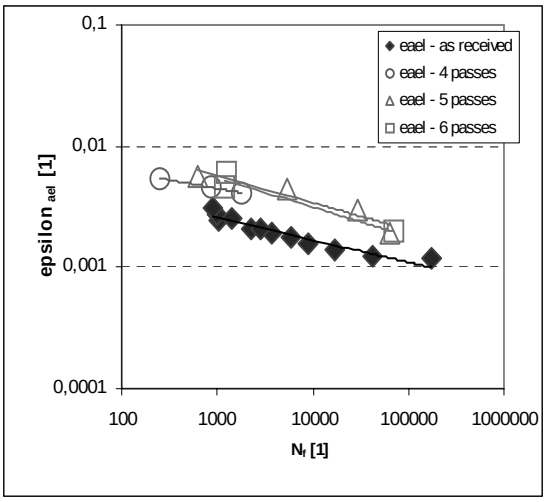

Fig. 18. Curves of low-cycle fatigue $\varepsilon_{ael} - N_f$

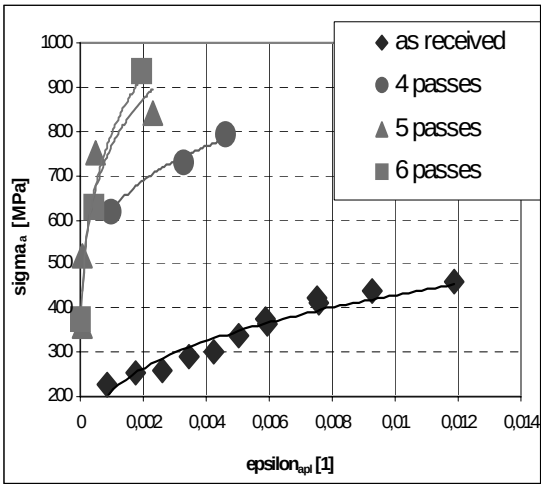

Fig. 19. Curves of dependence between the amplitude of stress σ_a - ε_{apl}

4. Conclusions

The following findings were obtained on the basis of experimental works:

Mechanical properties of the steel AISI 316 were determined by miniaturised tensile test, as well as by penetration test, selected samples were subjected to verification analysis of their chemical composition.

Basic mechanical properties of the steel AISI 316 were determined in dependence on number of passes. Series of experiments was also realised in order to verify influence of intensive magnetic field on structure and mechanical properties of this steel.

Fatigue behaviour of the steel AISI 316 was investigated after application of various number of passes through the ECAP tool, structural stability was preserved, however, fatigue service life in the area of timed fatigue strength decreased after application of ECAP.

It follows from these results that materials with ultra-fine grain after intensive plastic deformation by the ECAP technology show at fatigue loading in the mode of constant amplitude of deformation (low-cycle fatigue) shorter fatigue service life in comparison with initial state. Nevertheless, it is possible to regard as highly positive the fact, that ultra-fine grained structure shows comparatively good mechanical stability after fatigue test, which is given by the fact that grains in structure are so small, that they prevent forming of dislocation structure. This fact conforms to the findings published in the work, where it was observed and verified on Cu.

It can be predicted on the basis of obtained results that, contrary to low-cycle fatigue the ultra-fine grained material will manifest at fatigue load in the mode of constant amplitude of stress (high-cycle fatigue) higher fatigue characteristics, particularly fatigue limit.

Confirmation of this presumption requires, however, realisation of additional experimental works aimed at the area of high-cycle fatigue of investigated material AISI 316 and detailed investigation with use of electron microscopy of possible structural changes in material after tests of high-cycle fatigue.

Acknowledgements

The work was realised within the frame of solution of research plan VZ MSM 6198910013.

References

[1] M. Greger, R. Kocich, L.Čížek, Z. Muskalski, Mechanical properties and microstructure of Al alloys produced by SPD process, Proceedings of the 10th International Conference TMT'06, Barcelona, 2006, 253-256.
[2] M. Greger, R. Kocich, L. Čížek, L.A. Dobrzański, M. Widomská, B. Kuřetová, A. Silbernagel, The structure and mechanical properties of chosen metals after ECAP, Journal of Achievements in Materials and Manufacturing Engineering 18 (2006) 103-106.
[3] Q. Xue, X.Z. Liao, Y.T. Zhu, G.T. Gray, Formation mechanisms of nanostructures in stainless steel during high-strain-rate severe plastic deformation, Materials Science and Engineering 25 (2005) 252-256.
[4] A. Nowotmik, J. Sieniawski, M. Wierzbinska, Austenite decomposition in carbon steel under dynamic deformation conditions, Journal of Achievements in Materials and Manufacturing Engineering 20 (2006) 267-270.
[5] M. Jablonska, K. Rodak, G. Niewielski, Characterization of the structure of FeAl alloy after hot deformation, Journal of Achievements in Materials and Manufacturing Engineering 18 (2006) 107-110.
[6] Y. Fukuda, K. Ohishi, Z. Horita, T.G. Langdon, Processing of a low-carbon steel by equal-channel angular pressing, Acta Materialia 50 (2002) 1359-1368.
[7] L.A. Dobrzański, Engineering materials and materials design. Fundamentals of Materials Science and Physical Metallurgy, WNT, Warsaw, 2006 (in Polish).
[8] M. Borisova, S.P. Yakovleva, A.M. Ivanov, Equal channel angular pressing its effect on structure and properties of the constructional steel St3, Solid state Phenomena 114 (2006) 97-100.
[9] K. Rodak, M. Pawlicki, Microstructure of ultrafine-grained Al produced by severe plastic deformation, Archives of Material Science and Engineering 28/7 (2007) 409-412.
[10] J. Zrník, S.V. Dobatkin, L. Kraus, Influence of thermal condition of ECAP on microstructure evolution in low carbon steel, Materials Science Forum 558-559 (2007) 611-616.
[11] A. Hernas, G. Moskal, K. Rodak, J. Pasternak, Properties and microstructure of 12%Cr-W steels after long-term service, Journal of Achievements in Materials and Manufacturing Engineering 17 (2006) 69-72.
[12] M. Greger, R. Kocich, L. Čížek, L.A. Dobrzański, M. Widomská, Influence of ECAP technology on the metal structures and properties, Archives of Materials Science and Engineering 28/12 (2007) 709-716.
[13] D.H. Shin, C.W. Seo, J. Kim, K.T. Park, W.Y. Choo, Microstructures and mechanical properties of equal-channel angular pressed low carbon steel, Scripta Materialia 42/7 (2000) 695-699.
[14] V.M. Segal, Materials processing by simple sudar, Materials Science and Engineering 97/2 (1995) 157-164.
[15] I.H. Son, Y.G. Jin, Y.T. Im, Finite element investigation of fiction condition in equal channel angular extrusion, Journal of Achievements in Materials and Manufacturing Engineering 17 (2006) 285-285.
[16] B. Koczurkewicz, The model of prediction of the micro-structure austenite C-Mn steel, Archives of Material Science and Engineering 28/7 (2007) 421-424.
[17] R.Z. Valiev, A.V. Korznikov, R.R. Mulyukov, Structure and properties of ultrafine-grained materials produced by severe plastic deformation, Materials Science and Engineering 168/2 (1993) 141-148.
[18] Y. Iwahashi, J. Wang, Z. Horita, M. Nemoto, T.G. Langdon, Principle of equal-channel angular pressing for the processing of ultra-fine grained material, Scripta Materialia 35/2 (1996) 143-146.
[19] D.H. Shin, W.J. Kim, W.Y. Choo, Grain refinement of a commercial 0.15%C steel by equal-channel angular pressing, Scripta Materialia 41/3 (1999) 259-262.
[20] D.H. Shin, B.Ch. Kim, K.T. Park, W.Y. Choo, Microstructural changes in equal channel angular pressed low carbon steel by static annealing, Acta Materialia 48 (2000) 3245-3252.
[21] J. De Messemaeker, B. Verlinden, J. Van Humbeeck, Texture of IF steel after equal channel angular pressing (ECAP), Acta Materialia 53/5 (2005) 4245-4257.
[22] R. Kocich, M. Greger, A. Machačková, FEM simulation of extrusion by ECAP method on magnesium alloy AZ91, International Journal Computational Materials Science and Surface Engineering 1/4 (2007) 438-451.
[23] M. Greger, Microstructure of ultrafine-grained metals after ECAP, Proceedings of thr 11th International Conference TMT'2007, Hammamet, 2007, 1531-1534.
[24] M. Greger, R. Kocich, L. Čížek, L.A. Dobrzański, I. Jučička, Possibilities of mechanical properties and microstructure improvement of magnesium alloys, Archives of Materials Science and Engineering 28/2 (2007) 83-90.
[25] M. Greger, R. Kocich, L. Čížek Structure and low-cycle fatigue of steel AISI 316 after ECAP, Journal of Achievements in Materials and Manufacturing Engineering (2008) (in print).